Materials Testing 2026; 68(4): 700–714 DE GRUYTER

Materials Modelling

Mehmet Özer, Kaan Ferikel, Fatih Balıkoğlu, Tayfur Kerem Demircioğlu, İbrahim Kutay Yilmazçoban* and Can Çivi

Ballistic performance of multi-layered armor combinations under 7.62 × 51 mm FMJ bullet impact

https://doi.org/10.1515/mt-2025-0177
Published online January 23, 2026

Abstract: This work performed a nonlinear numerical analysis of Armox 500T and Hardox 450 armor steels, Kevlar 29/epoxy laminate, and aluminum honeycomb materials under ballistic conditions, validating the results via experimental data. The ballistic performance of 20 distinct armor configurations was investigated, including monolithic steel, steel-composite, and steel-composite-honeycomb panels produced by various material arrangements. Ballistics tests were conducted using 7.62 × 51 mm full metal jacket bullets with a muzzle velocity of 838 ± 15 m s^{-1} under the NIJ 0108.01 III protection level standard. The effect of Kevlar29/epoxy layer thickness in multi-layered panels was examined extensively. The results showed that the ballistic performance of the composite armors was significantly improved due to the combination of monolithic steel plates with Kevlar 29/epoxy and aluminum honeycomb layers. Steel-Kevlar 29/epoxy and steel-Kevlar 29/epoxy-honeycomb multi-layered plates provide identical ballistic protection to monolithic steel counterparts while being 51 wt.% and 57 wt.% lighter than monolithic steel armor. Comprehensive finite element simulations of the ballistic impact events were conducted to elucidate the phenomena of defeat and penetration with greater precision.

Keywords: armor steels; aluminium honeycomb; ballistic test; composite; finite element

***Corresponding author: İbrahim Kutay Yilmazçoban**, Mechanical Engineering, Sakarya University, Sakarya, Türkiye,
E-mail: kyilmaz@sakarya.edu.tr. https://orcid.org/0000-0002-9886-5533
Mehmet Özer, Fatih Balıkoğlu and Tayfur Kerem Demircioğlu, Mechanical Engineering, Balikesir University, Balikesir, Türkiye. https://orcid.org/0000-0003-3836-5569 (F. Balıkoğlu)
Kaan Ferikel, Mechanical Engineering, Sakarya University, Sakarya, Türkiye. https://orcid.org/0009-0006-1616-0174
Can Çivi, Mechanical Engineering, Manisa Celal Bayar University, Manisa, Türkiye

1 Introduction

All armored vehicles require a balance in ballistic protection, providing adequate defense while minimizing weight. Therefore, vehicle armor design meets inconsistent needs; there is a common desire to reduce structural weight to enhance maneuvering and decrease fuel consumption; however, more mass is required to improve armor protection and payload capacity [1]. Developing the ability to withstand high-caliber bullets and reduce weight is a crucial objective for applications in the military. Hardened steel plates are frequently employed as armor against the ballistic threat of rifle bullets and fragments with similar destructive power. The armor can be characterized by steels that exhibit high ductility, as well as high hardness and strength values [2], [3]. In addition to these attributes, it is crucial to consider its superior loading capacity, low price compared to most other armor materials, and ease of shaping [4]. The higher density of steel offers a drawback compared to some metals, ceramics, and composite materials. Also, in recent years, with increasing demand for lighter structures, the use of steel in ballistic applications has gradually reduced, while the popularity of multi-layered armored structures has increased [5].

The ballistic impact resistance of multi-layered armors produced with different materials, including armor steels, aluminum, ceramics (SiC, B_4C, Al_2O_3), ultra-high molecular weight polyethylene (UHMWPE) (Dyneema®), and aramid (Kevlar®), has been investigated in the literature. Senthil and Iqbal [6] investigated the ballistic performance of layered configurations of Armox 500T, mild steel, and Al 7075-T651 sheets against 7.62 AP (Armour Piercing) bullets with a muzzle velocity of 818 m s^{-1} in normal and oblique shots. As the best configuration, the authors suggested using low ductility-high strength Armox 500T in the front layer and high ductility-low strength Al 7075-T651 or medium strength-medium ductile mild steel in the middle and rear layers. Paman et al. [7] studied the optimal order and thickness of the material layers of a multi-layered armor module by numerical simulation and ballistic experiments to provide both ballistic resistance against 7.62 armor-piercing bullets and minimum weight. The authors applied the methodology to three metal alloys: Armox-500T, Ti-6Al-4V, and Al-2024. They first carried out numerical simulations to examine the ballistic impact behavior of these three materials using the AUTODYN-3D code. Ballistic experiments showed that the Armox-500T/Ti-6Al-4V/Al-2024 array, with 5.5, 8.5, and 13 mm thicknesses, respectively, has the best resistance against 7.62 mm armor-piercing bullets at an initial velocity of 840 ± 10 m s^{-1}. It was found that the composite module was more efficient than Armox-500T and Al-2024 in terms of weight and had better performance than Al-2024 in terms of armor thickness. Peng et al. [8] compared the ballistic resistance of hybrid layers developed with SiC, B_4C ceramic layers, Dyneema®, aramid (Kevlar®), and compressed wood materials.

Test samples were subjected to field ballistics tests with 7.62 mm (×39 mm) bullets at a speed range of 806–887.5 m s^{-1}. According to ballistic results, the B_4C-Dyneema composite panel provided the best ballistic performance with the lowest areal density and thickness. Although compressed wood is one of the lightweight materials, it was observed that its ballistic performance and energy absorption are poor. Palta et al. [9] created nonlinear finite element (Fe) models of Weldox 700E steel and Kevlar 129/epoxy plates and. compared numerical solutions to experimental results. A parametric study using numerical models was prepared to investigate the ballistic performance of monolithic steel and multi-layer plates following NATO Level I or EN1063 BR5 standards. It has been demonstrated that the double-layer steel plate with the thicker back layer has a higher ballistic resistance than the one with the thinner back layer. For double-layer hybrid plates with the same steel layer thickness, the plate using Kevlar on the back layer had better protection and was more efficient. The steel-Kevlar-steel configuration for three- and four-layer plates was the most successful of all multi-layer hybrid plates. It was also observed that using a single layer of Kevlar provides better ballistic protection than using two layers of Kevlar. Kraus et al. [10] numerically examined the interaction of the heterogeneous structure they created by placing steel and ceramic plates in the Kevlar pocket against ballistic impact. Based on direct numerical simulation, they concluded that the steel+B_4C armor plate has the best weight and size parameters. Kartikeya et al. [11] ballistically tested a steel/ultra-high molecular weight polyethylene composite armor system against a 7.62 × 39 mm hardened steel core (HSC) projectile. The steel/UHMWPE composite structure with a 3 mm thick high hardness steel (HHS) plate protected against 7.62 × 39 mm HSC bullets fired at a speed of 700 m s^{-1}.

The ballistic resistance of aluminum honeycomb structures under the influence of fragments with different geometries was investigated in the literature. Using honeycomb structures has significantly contributed to the sandwich structure's ballistic impact response by reducing the residual velocity, kinetic energy, and damaged area. Although the ballistic performance of aluminum honeycomb structures has been studied in sandwich structures [12]–[15], this work evaluated the contribution of armor steel and Kevlar29/epoxy laminate plate to energy absorption.

This study aims to define multi-layered armor structure arrays that are lighter while maintaining ballistic resistance and can give a better result considering the armor combinations to replace monolithic and high-area-weight steel armor. To this end, it is planned to replace monolithic Armox 500T steel armor plates with multi-layer steel, Kevlar29/epoxy, and aluminum honeycomb armor panels that meet the NIJ 0108.01 Level III protection requirement for light armored vehicles. The combination of armor steel with aluminum honeycomb and Kevlar 29/epoxy composite highlights the innovative side of this work. For this level of protection, multi-layered plates were manufactured to provide protection against 7.62 × 51 mm full metal jacket (FMJ) bullets with a velocity of 838 ± 15 m s^{-1}. Firstly, the finite element model of the target plates, including material modeling, was prepared using LS Dyna® software. Then, a parametric study evaluated the ballistics tests of 20 hybrid plate configurations with different thicknesses and layer arrangements; the perforation, backface deformation, and failure mechanisms were compared with the experimental results. The test results showed that the 4A14K sample had the highest specific energy absorbed value.

2 Materials and methods

2.1 Armour materials

A parametric study with 20 different armor plate configurations was conducted to determine whether the targets produced within the scope of the study fulfill the protection level specified in the NIJ STD-0108.01 Level III standard [16]. The steel layers used in all configurations are made of Armox 500T and Hardox 450 steel. In addition, Kevlar 29/epoxy composite and aluminum honeycomb panels were combined with steel plates to form hybrid plates. Steel-composite and multi-layer hybrid plates were studied experimentally versus numerically to understand the effects of thickness configurations for monolithic steel. The thickness of all target armor structures varies between 4 and 24.8 mm. In the abbreviation of all armor plates, the thickness is expressed in mm for steel and aluminum honeycomb panels and in layers for Kevlar 29/epoxy composite sheet. The code

4A18K10B, for instance, indicates a hybrid armor plate with 4 mm Armox 500T steel, 18 layers of Kevlar 29/epoxy composite, and a 10 mm aluminum honeycomb panel. The chemical compositions of the two steels from the SSAB firm are presented in Table 1, and their mechanical properties are detailed in Table 2. The configuration of all armor plates included in the experimental study is illustrated in Table 3. The letters "A", "H", "B", and "K" in the sample abbreviations refer to Armox500T, Hardox450, aluminum honeycomb, and Kevlar29/epoxy layers, respectively. The numbers before the Kevlar29/epoxy layer indicate the number of fabric layers. Other numbers denote each plate's thickness in millimeters.

Plain woven Kevlar® 29 fiber, woven from lightweight, water-repellent, and high-quality para-aramid fibers with an area weight of 200 g m^{-2}, utilized in the fabrication of ballistic vests, was used to produce the aramid–epoxy composite laminate. MGS lamination epoxy set (Resin: L285, Hardener: H285) was used as a matrix to manufacture composite panels. Production was conducted using the hand lay-up method, and the mixture was impregnated into the fibers layer by layer with a brush, following the instructions in the MGS lamination epoxy set. The resin and hardener ratio is 100:40. Each layer of lamination aluminum roller is used to evacuate the air gaps. The aluminum honeycomb plate at the rear of the armor plate array has an area weight of 5.0 kg m^{-2} and a bending value of 21,900 kN m^2 m^{-1}. Moreover, it is a lightweight panel featuring a cell diameter of 9 mm and a foil thickness of approximately 0.20 µm.

2.2 Full metal jacket bullet

According to NIJ STD-0108.01 Level III, a 7.62 × 51 mm NATO FMJ bullet was selected with a speed standard of 838 ± 15 m s^{-1}. Figure 1 illustrates the 7.62 × 51 mm FMJ bullet utilized in the parametric investigation, whereas Table 4 indicates the characteristics of the 7.62 × 51 mm FMJ bullet.

2.3 Ballistic tests

Ballistics tests were conducted in the indoor shooting range of ZSR corporation located in Balikesir province, Türkiye. The closed range had an air conditioning system, and the ambient temperature was maintained at 22 °C during the experiments. This ambient temperature falls between the 20–28 °C range specified in the standard. Armor plate targets were hit with the Prototypa brand gun in Figure 2a in this range, utilizing the 7.62 × 51 mm caliber FMJ bullet manufactured by this company. The ballistic test setup was set at level III protection within the scope of the "NIJ 0108.01 Ballistic Resistant Protective Materials" standard (Figure 2b). Five shots were completed on the test plates in compliance with the standard. A single comprehensive photograph illustrating the damage caused by the bullets on the plate was identified, and the damage status of the relevant plate was shown during the experiments. The target plates were not supported using clay as recommended in the standard (Figure 2c). The distance between the test plate and the gun barrel was 15 m at protection level III. In ballistic laboratory tests, bullet exit velocities were not measured due to the risk of being detrimental to ZSR's velocity measuring apparatus; just muzzle exit velocities were recorded. The exit velocity values obtained from finite element analyses are presented in this study.

Table 2: Mechanical properties of Armox 500T and Hardox 450 steels [17].

Properties	Symbols	Unit	Armox 500T	Hardox 450
Hardness	HBW	–	480–540	420–475
Impact toughness at −40 °C (Charpy)	KV	J	32	35
Yield strength	$R_{p0.2}$	MPa	1,250	1,200
Ultimate strength	R_m	MPa	1,450–1,750	1,400
Elongation	A_5	%	8	10
	A_{50}	%	10	–

A5 (Extensometer range of 5 mm), A50 (Extensometer range of 50 mm).

2.4 Finite element modeling

2.4.1 Mesh procedure

Initially, a CAD model of the ammunition was made by utilizing measurements from an actual 7.62 × 51 mm FMJ bullet. Half of the bullet was meshed using eight-node brick elements with limited integration and stiffness-based hourglass

Table 1: The amount of alloying elements in Armox 500T and Hardox 450 steels [17].

Elements	C	Si	Mn	P	S	Cr	Ni	Mo	B
Armox 500T	0.32 %	0.40 %	1.20 %	0.015 %	0.010 %	1.01 %	1.18 %	0.70 %	0.005 %
Hardox 450	0.26 %	0.70 %	1.60 %	0.025 %	0.010 %	1.40 %	1.50 %	0.50 %	0.005 %

Table 3: Target plate configurations.

Configuration	Geometry	Code	Total thickness (mm)	Layers	Areal density ρ_A (kg m^{-2})
Monolithic steels	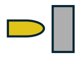	4A	4.0	1 × 4 mm Steel	7.83
		4H	4.0	1 × 4 mm Steel	8.13
		6A	6.0	1 × 6 mm Steel	7.83
		6H	6.0	1 × 6 mm Steel	8.13
Double-layered		4A6K	6.7	1 × 4 mm Steel +1 × 2.4 mm Kevlar29/epoxy	5.18
		4A8K	7.6	1 × 4 mm Steel +1 × 3.6 mm Kevlar29/epoxy	4.72
		4A10K	8.5	1 × 4 mm Steel +1 × 4.5 mm Kevlar29/epoxy	4.35
		4A12K	9.4	1 × 4 mm Steel +1 × 5.4 mm Kevlar29/epoxy	4.05
		4A14K	10.3	1 × 4 mm Steel +1 × 6.3 mm Kevlar29/epoxy	3.83
		4A16K	11.2	1 × 4 mm Steel +1 × 7.2 mm Kevlar29/epoxy	3.60
		4A18K	12.1	1 × 4 mm Steel +1 × 8.1 mm Kevlar29/epoxy	3.43
		4H24K	14.8	1 × 4 mm Steel +1 × 10.8 mm Kevlar29/epoxy	3.12
Triple-layered	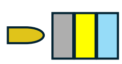	4A6K10B	16.7	1 × 4 mm Steel +1 × 2.4 mm Kevlar29/epoxy +1 × 10 mm Honeycomb	3.70
		4A8K10B	17.6	1 × 4 mm Steel +1 × 3.6 mm Kevlar29/epoxy +1 × 10 mm Honeycomb	3.57
		4A10K10B	18.5	1 × 4 mm Steel +1 × 4.5 mm Kevlar29/epoxy +1 × 10 mm Honeycomb	3.46
		4A12K10B	19.4	1 × 4 mm Steel +1 × 5.4 mm Kevlar29/epoxy +1 × 10 mm Honeycomb	3.36
		4A14K10B	20.3	1 × 4 mm Steel +1 × 6.3 mm Kevlar29/epoxy +1 × 10 mm Honeycomb	3.26
		4A16K10B	21.2	1 × 4 mm Steel +1 × 7.2 mm Kevlar29/epoxy +1 × 10 mm Honeycomb	3.18
		4A18K10B	22.1	1 × 4 mm Steel +1 × 8.1 mm Kevlar29/epoxy +1 × 10 mm Honeycomb	3.10
		4H24K10B	24.8	1 × 4 mm Steel +1 × 10.8 mm Kevlar29/epoxy +1 × 10 mm Honeycomb	2.94

control since the bullet was axisymmetric around the longitudinal axes. The mesh structure of the bullet-armor elements was created manually within the LS-DYNA® software. The numerical model included 89,635 elements for the 7.62 × 51 mm FMJ bullet, with mesh diameters varying from 0.07 to 0.25 mm. The bullet's striking location to the armor plate is where the penetration occurs; hence, it is represented by a finer mesh structure. A half-model was created for each target using the same element type as the bullet. The mesh sizes in the target plate were assigned between 0.25 and 0.625 mm. This modeling technique minimizes processing time needs while maintaining an optimal system balance. For Armox 500T and HARDOX 450 steels, 276,480 elements were defined. The number of elements in the composite layers ranged from 17,280 to 829,440, depending on the number of layers. Eight hundred two thousand seven hundred thirty elements were assigned for 0.2 mm mesh size in the honeycomb structure. Figure 3 shows the boundary

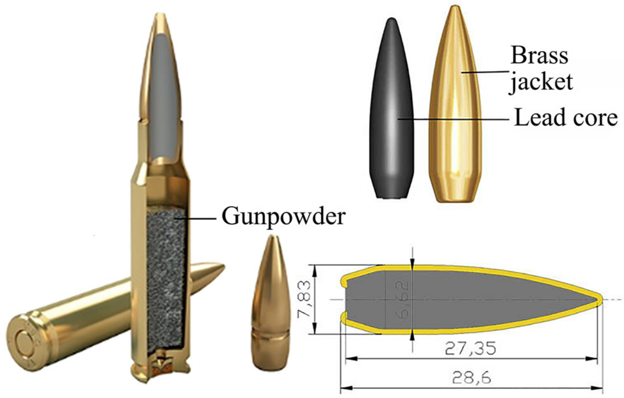

Figure 1: 7.62 × 51 mm FMJ bullet and dimensions in the experimental and numerical study.

Table 4: Technical specifications of 7.62 × 51 mm FMJ ammunition.

Bullet	7.62 mm FMJ
Core diameter	7.83 mm
Core weight	9.60 g
Cartridge case weight	11.84 g
Length	28.6 mm
Gunpowder quantity	2.768 ± 0.005 g

condition where the armor plates remain fixed at each degree of freedom along their four side surfaces.

Two different simulations were conducted in µthe 6 mm Armox 500T test to determine the optimal element size, using element sizes of 0.5 mm and 0.25 mm for all components. In the contact relations, all parameters remained constant except for the contact stiffness and contact step duration, which depend on the element size. The experimental results were compared with those obtained by varying the mesh size. The element size of 0.5 mm provided a 16-fold decrease in solution time, but the deformation value on the back surface of the plate was 14.7 wt.% higher than the experimental result. On the other hand, it was determined that although the element size was 0.25 mm, it responded closer to the experimental results and had a 6.1 wt.% lower back deformation depth. The mesh size used for the target plate is consistent with the literature [18], [19]. The cause of this phenomenon is the variance of about 15 m s^{-1} in the velocity of the bullets used in the experiment, as indicated in the relevant standard and by the manufacturer.

2.4.2 Material model

The MAT_015_JOHNSON_COOK (Ls-Dyna Software description) [20] material model was used for the steels because of its excellent precision and stable performance, not affected by dynamic fluctuations in deformation rate for explicit dynamic conditions. This viscous-plastic material model includes the effects of temperature, strain rate, and strain hardening [21], [22]. Table 5 shows the material parameters of Armox 500T and Hardox 450 armor steel plates, which are also obtained from the literature [23], [24].

The macro-homogeneous approach for modeling composite laminates is widely used in the literature [25]–[29]. In this method, each layer is assumed to be a homogenous material, with no difference between the yarns and the matrix; hence, the physical characteristics are homogeneous, the same at all points in the layer, but with orthotropic mechanical properties. In addition, the fabric structure has two perpendicular in-plane directions with the same mechanical characteristics within the plane owing to symmetry, for example, equal elastic modulus and strength values, but different mechanical properties out of the plane.

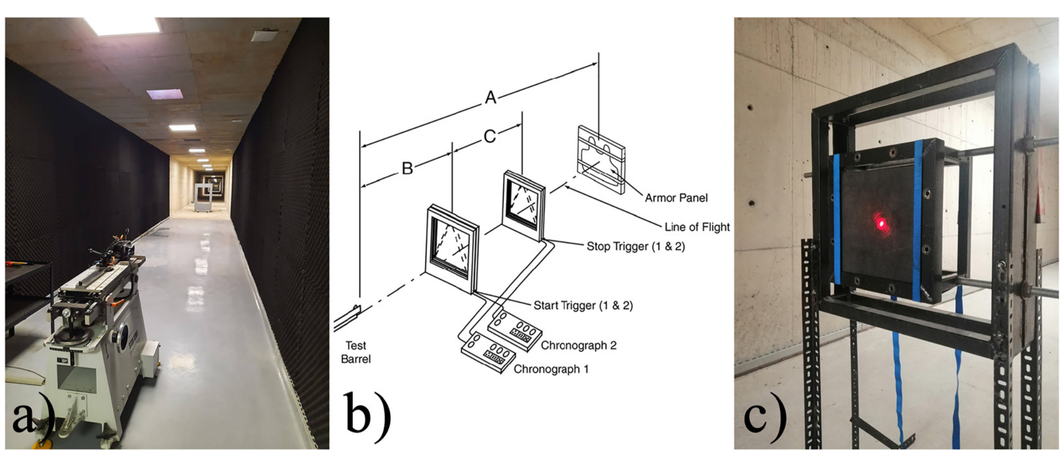

Figure 2: Ballistics Testing Laboratory. a) Closed range and prototype brand shooting apparatus belonging to ZSR A.Ş. Company, b) schematic illustration of the test standard (NIJ STD-0108.01 level III), c) target plate holder.

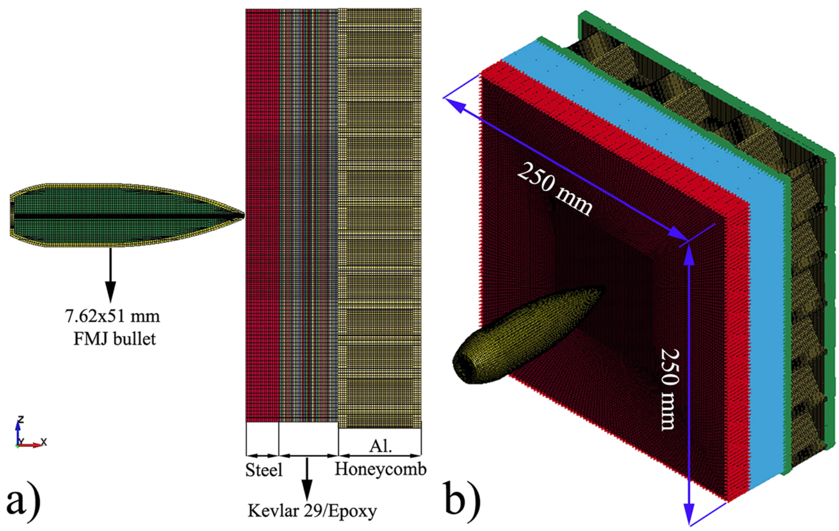

Figure 3: Details of the finite element model, a) sectional view of the finite element model of the 4A18K10B armour plate b) image of the zero-degree-of-freedom points of the armour plate.

Moreover, this method allows the introduction of preferred delamination in planes. As the number of sub-laminates increases, the number of elements in the problem increases, thus increasing the total computational time required to solve the problem [11], [30]. The modeling of Kevlar29/epoxy laminates used the MAT_058_LAMINATED_COMPOSITE_FABRIC (Ls-Dyna Software description) material model [20]. This material model includes nonlinear material behavior, damage initiation, and failure under impact or higher strain rates, which is essential for the study. These characteristics of the material model are appropriate for crash simulations and ballistic impact analysis, where progressive damage through the layers is vital for precise ballistic performance prediction. The damage evolution in this material model involves progressive degradation of the material's stiffness and strength as damage accumulates due to tensile, shear, and bending loads. The model uses failure criteria based on stress or strain in the fiber and matrix direction, initiating damage once thresholds are exceeded by eroding a node or an element. The mechanical properties of the Kevlar 29/epoxy composite material are given in Table 6.

Table 5: Material properties for Armox 500T [22] and Hardox 450 [23] armor steels.

Mechanical properties	Hardox 450	Armox 500T
Density ρ (kg mm^{-3})	8.13E-06	7.83E-06
Shear modulus G (GPa)	71.80	79.60
Yield stress A (GPa)	1.0690	0.3850
Hardening constant B (GPa)	0.9371	1.4050
Hardening exponent n	0.3438	0.0263
Strain-rate sensitivity constant c	0.0911	0.0870
Temperature sensitivity exponent m	1.0000	1.0440
Failure parameters		
D1	1.6900	0.0680
D2	−0.2843	5.3280
D3	−0.1837	2.5540
D4	0.0600	0.0000
D5	0.0000	0.0000

Table 6: Material properties for Kevlar 29/epoxy [31].

Material parameters	Values		Values
Density ρ (kg mm^{-3})	1.26E-06	XC (X Compressive strength)	0.1850
EA (Elasticity modulus X)	17.23	XT (X Tensile strength)	0.4050
EB (Elasticity modulus Y)	17.23	YC (Y Compressive strength)	0.1850
EC (Elasticity modulus Z)	10.40	YT (X Tensile strength)	0.4050
PRBA (Poisson ratio XY)	0.20	ZC (X Compressive strength)	0.0869
PRCA (Poisson ratio ZX)	0.12	ZT (Z Tensile strength)	0.0345
PRCB (Poisson ratio ZY)	0.12	SC (XY Shear strength)	0.0770
GAB (Shear modulus XY)	5.51	SC23 (YZ Shear strength)	0.8980
GBC (Shear modulus YZ)	3.30	SC31 (ZX Shear strength)	0.8980
GCA (Shear modulus ZX)	3.30	SLIMT3	0.5000
SLIMT1	0.50	SLIMC3	0.8000
SLIMC1	0.80	SLIMS23	0.5000
SLIMT2	0.50	LSIMS31	0.5000
SLIMC2	0.80	EFFEPS (Compound strain at fracture point)	1.6870
SLIMS	0.50	VOLEPS (Volumetric strain at failure limit)	−0.6964
SOFT	0.90	EPSSH (Shear stress at failure limit)	0.6033

The MAT_098_SIMPLIFIED_JOHNSON_COOK material model card was chosen for modelling a bullet element, and the honeycomb layer faces since it offers a highly accurate solution while optimizing processing power and solution time. This model applies to problems where strain rates vary dramatically. MAT_026_HONEYCOMB was used to simulate the hexagonal profiled internal structure of the honeycomb panel [20].

2.4.3 Contact assignments

The "Step-Duration" calculation included in the Ls-dyna software via the CONTROL_TIMESTEP card was set to 0.85 to enhance the efficacy of both the analysis and the contact relationship, given the increased bullet velocity. Furthermore, the "HOURGLASS" energies and CONTROL_ENERGY cards were activated to obtain more realistic solutions. In addition, by setting the "ECDT" option to 1 on the CONTROL_CONTACT card, the influence of "ERODING_CONTACT" on the analysis step time was minimized. The ERODING_SURFACE_TO_SURFACE [20] card was selected to define the interaction between the bullet components and the armor plates and the bullet's penetration toward the target inside the program. Due to an incorrect operation of ERODING_SURFACE_TO_SURFACE without activating optional cards, choices A, B, and C from the optional cards were activated. The SOFT option was chosen as 2 (Reaction formula derived from pinball contact segments). To enhance accuracy, the "contact step-time," utilized exclusively by the SOFT 2 contact algorithm, and the "contact stiffness," applicable to all contact algorithms, were manually computed and specified within the program for the designated contact relationships between each component. The default SOFT value of 0 was initially computed and established in the "SLDSTF" section. The equation for SOFT = 2 was calculated and recorded in the "DTSTIF" section. Due to the bullet's high velocity, "MAXPAR" (Maximum Parametric Coordinate Search in Segment Search) was increased from 1.025 to 1.12. The DEPTH option was set to 5 (which checks surface and edge contact points). The ERODING_SINGLE_SURFACE card contact algorithms established the contact relation between the armor plates and the bullet components. The TIED_SURFACE_TO_SURFACE [20] contact algorithm card was used to create the lamination connection between the layers of the aramid/epoxy laminate composite.

3 Results and discussion

3.1 Monolithic steel panels

First, four monolithic steel panels of identical thickness were evaluated: 4A, 4H, 6A, and 6H. As anticipated, the 4A sample with a higher hardness value had a much lower residual velocity compared to the 4H sample (Figure 4a). Samples 4A and 4H both suffered from petalling damage mode (Figure 4c). Conversely, the 6A sample demonstrated ballistic resistance with a reduced backface deformation compared to the 6H sample however neither of the panel's experienced complete perforation failure mode. As anticipated, the back surface bulging damage mechanism was seen in the 6A and 6H steel samples (Figure 4b). The backface deformation in the monolithic 6A sample was less than that in the 4A sample (Figure 4b and c).

3.2 Double-layered panels

Plates comprising double-layer steel and composite layers with total thicknesses between 6.7 mm and 14.8 mm were

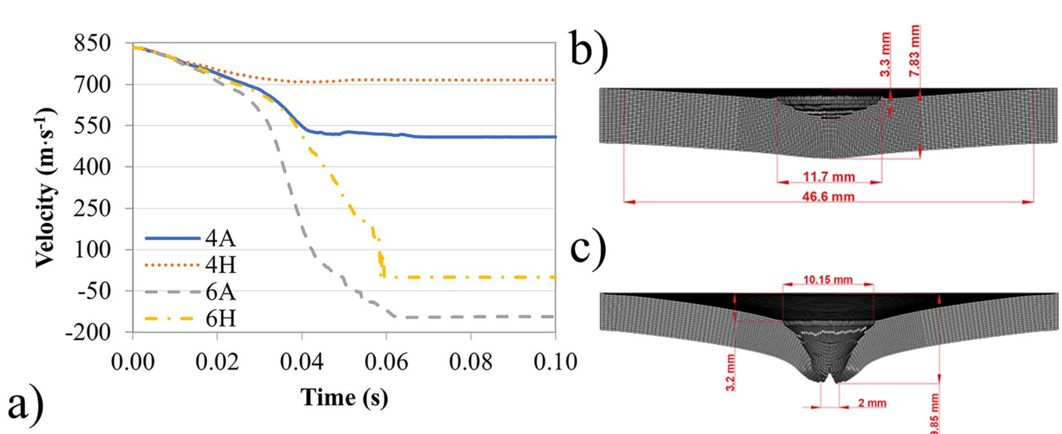

Figure 4: Ballistic evaluations for monolithic test panels. a) Bullet initial and residual velocity – time graphs of monolithic steel armor panels, post impact deformations of b) sample 6A, c) sample 4A.

fabricated (see Table 3), and the effect of the Kevlar29/epoxy composite layer structure was evaluated. Due to the occurrence of complete perforation failure in 4 mm thick monolithic steels, the goal is to address this problem by implementing multi-layered structures. The 4H24K hybrid plate, considering double-layered armor, using Hardox 450 steel on the impact surface, failed to show ballistic protection, resulting in complete perforation damage. The front steel layer of the 4A24K sample failed via petalling, while the rear Kevlar 29/epoxy plate fractured completely. Hence, it was not practicable to suggest double-layer panel armor composed of Hardox 450 steel instead of the 6H plate for ballistic protection. For armor plates with Armox 500T on the impact surface, composite layers ranging from 6 to 18 layers of aramid-epoxy were used. The 4A14K sample was found to provide ballistic protection.

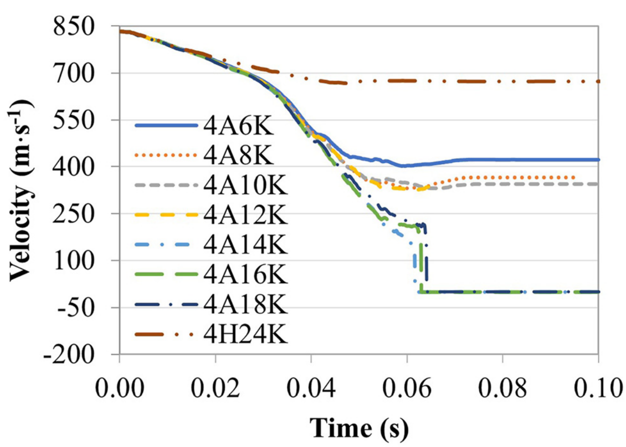

Figure 5: Bullet initial and residual velocity – time graphs of steel-composite armour panels.

The test results for the 4A6K, 4A8K, 4A10K, and 4A12K samples showed complete perforation failure. Reducing the Kevlar layer number in completely perforated samples produced a higher residual speed value. The 4A14K sample, which provides a weight benefit, may be preferred over the 6A panel. As expected, the 4A16K and 4A18K samples showed better ballistic protections considering the thickness increment. Adding the Kevlar 29/epoxy layer facilitated increased friction and better energy absorption during the passage of the bullet core. Figure 5 shows the residual velocity changes of eight configurations. In panels with complete perforation, the bullet residual velocity decreased as the thickness of the Kevlar/epoxy layer increased.

The front steel plate will absorb most of the bullet's kinetic energy through petalling failure. The Kevlar/epoxy plate absorbed the bullet's residual kinetic energy via punching, fiber fracture, and delamination. The bullet remained in the Kevlar/epoxy layers and was eroded and distorted. This instance demonstrates that layer thickness, combination type, and arrangement form in double-layer plate plans can all influence material performance. The visual of the damage caused by the ballistic test of the double-layered critical 4A14K sample is given in Figure 6. Cracks and radial fractures were observed on the rear surface of the front steel layer of the 4A14K sample as a result of bulge damage.

Figure 7 presents the Von Mises stress distribution of the thinnest and thickest steel-composite 4A6K and 4A12K samples, respectively, when the complete perforation occurred under the impact of a bullet. The stress values in

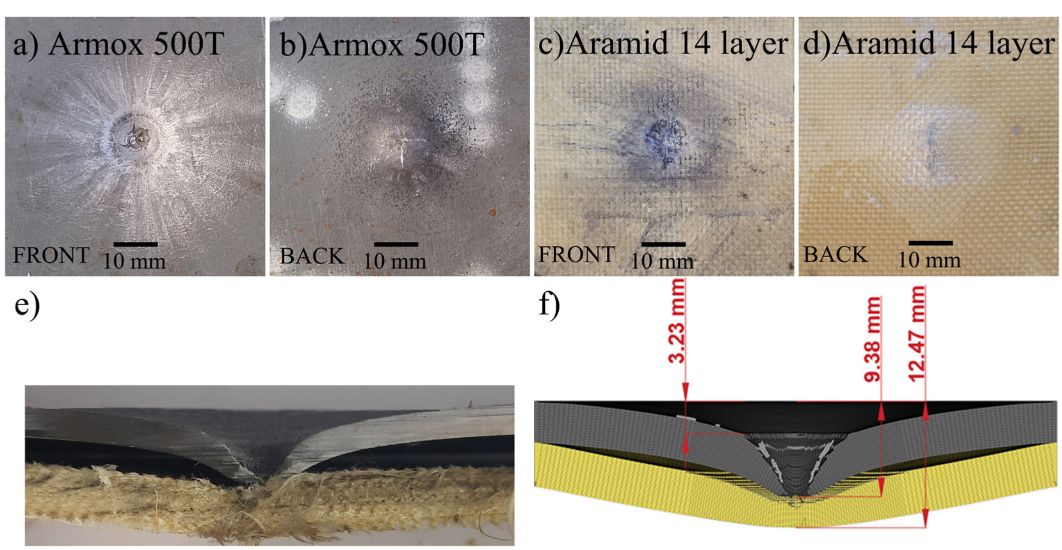

Figure 6: Damage image of double-layer 4A14K plate after impact, a) Armox 500T front view, b) Armox 500T rear view, c) composite front view, d) composite rear view, e) damage view of finite element analysis.

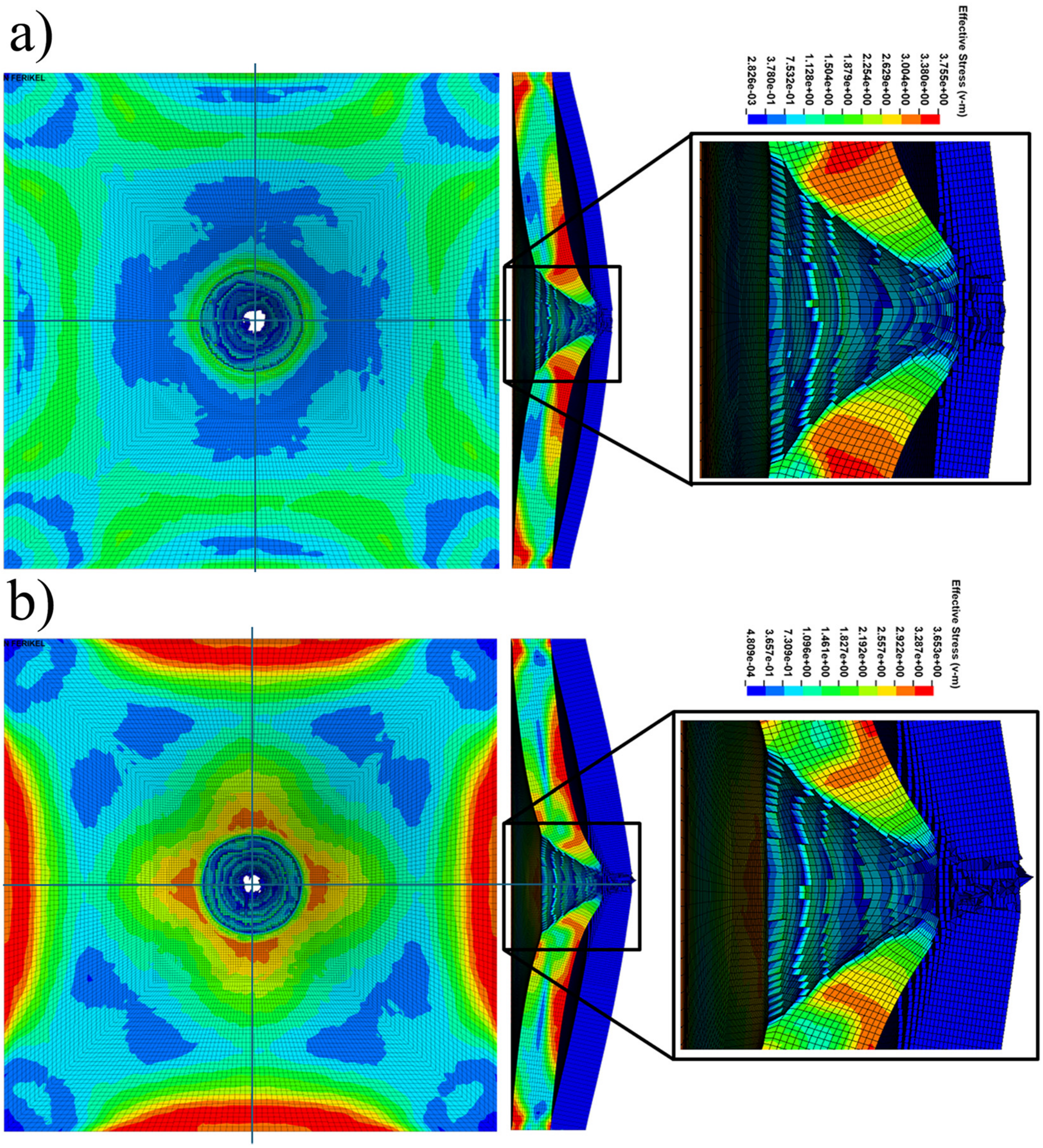

Figure 7: Von Mises stresses (in Pa) of steel-composite plates, a) 4A6K and b) 4A12K.

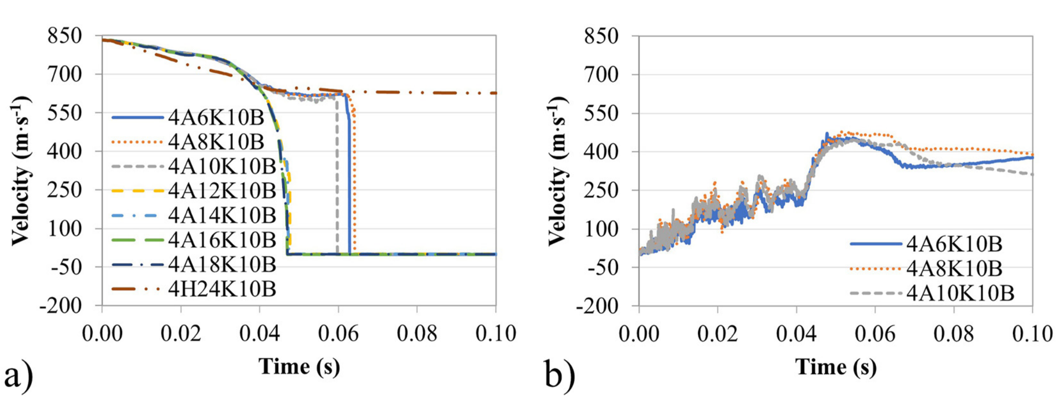

Figure 8: Ballistic evaluations for triple-layered test panels. a) Bullet initial and residual velocities, b) velocity values of the steel fragment piercing the multi-layer panels.

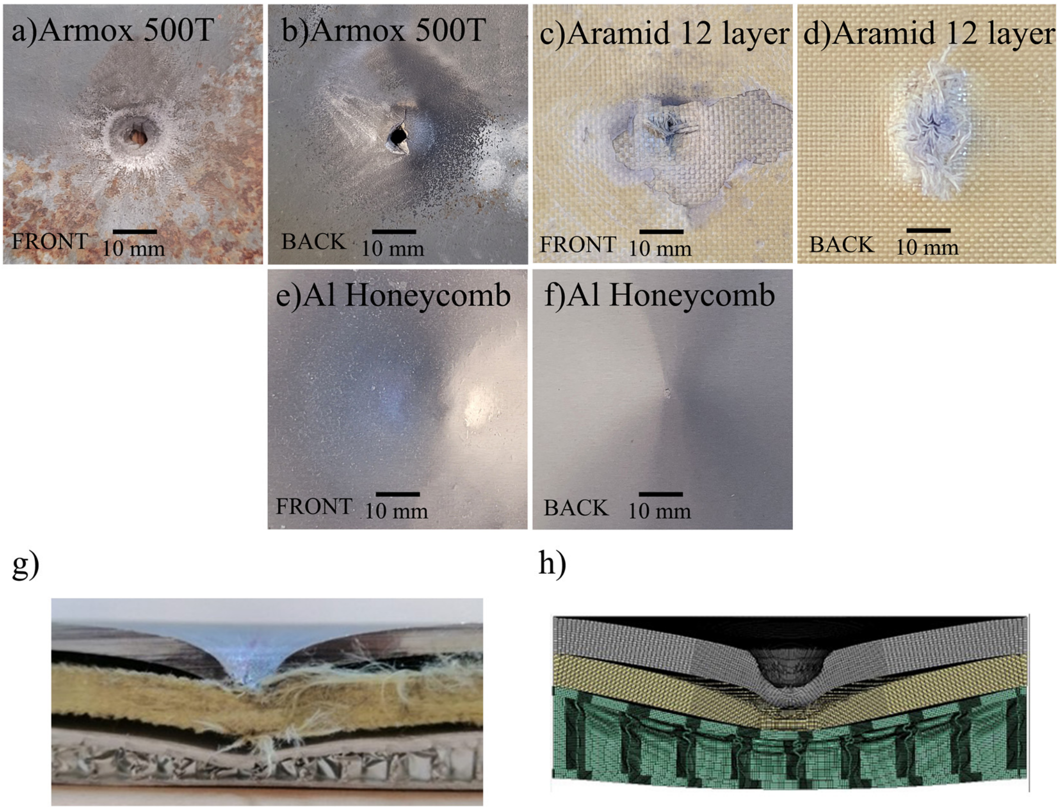

Figure 9: Post-damage images of the 4A12K10B sample, a) Armox 500T front view, b) Armox 500T rear view, c) Kevlar 29/epoxy front view, d) Kevlar 29/epoxy rear view, e) aluminum honeycomb front view, f) aluminum honeycomb rear view, g) post-impact photograph, h) finite element analysis damage sectional view.

the steel plate increased as the number of Kevlar29/epoxy layers increased. Following this result, an aluminum honeycomb was applied in the following step to increase wall thickness in triple-layered panels and assess its ballistic resistance contribution. Moreover, the failure mechanisms of the 4A6K and 4A12K samples were also examined. The main damage mechanisms resulting from this impact region are petalling and cracking in the steel plate's rear, fiber breakage, and delamination failures in Kevlar29/epoxy layers.

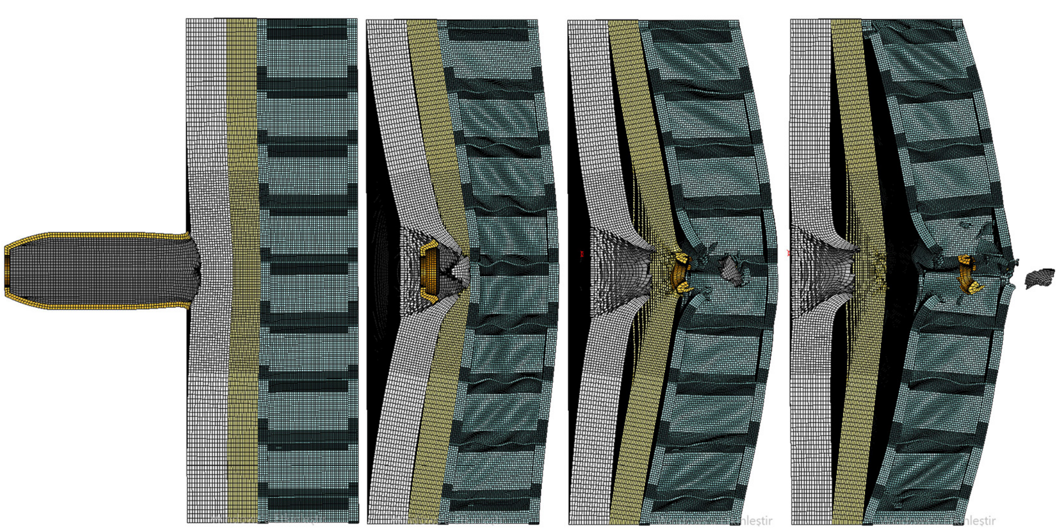

Figure 10: Post-impact damage image of the 4A10K10B sample.

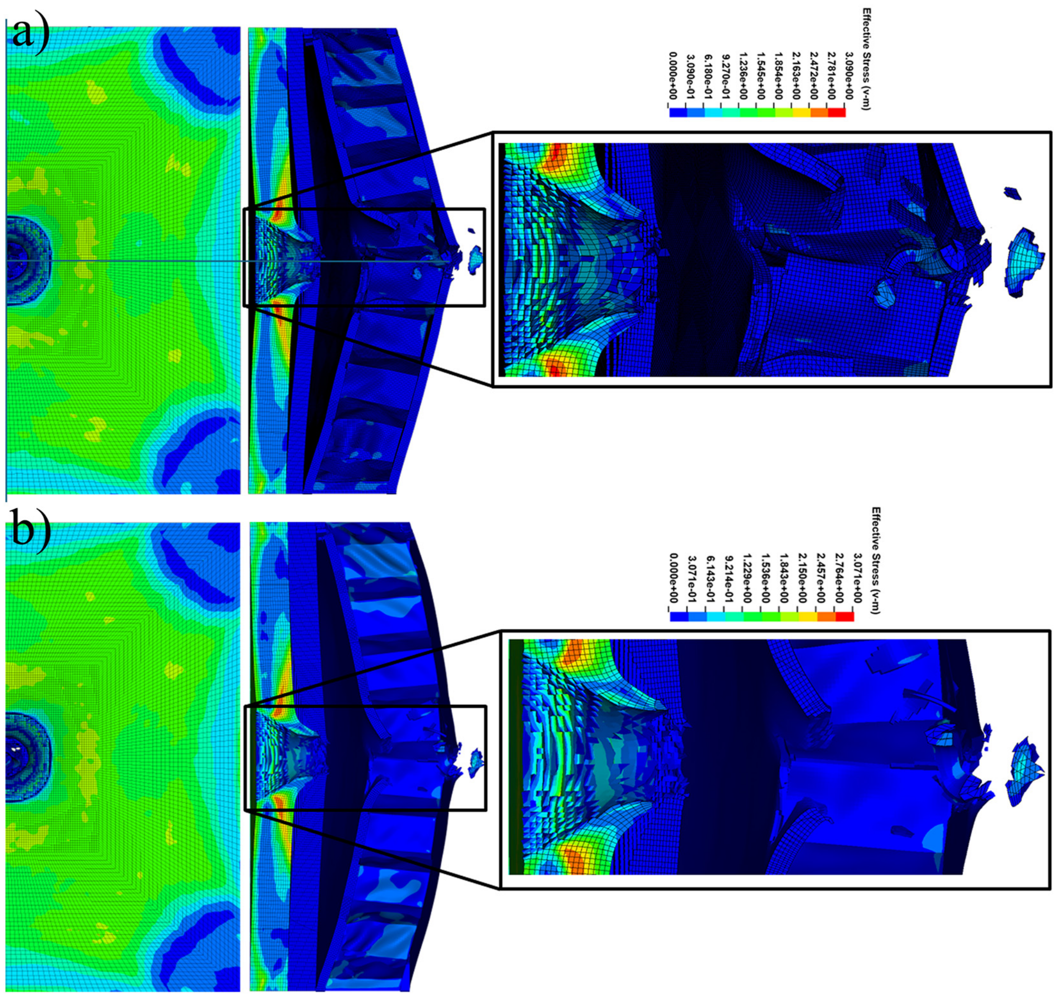

Figure 11: Von Mises stresses (in Pa) of triple-layered panels, a) 4A6K10B and b) 4A10K10B.

3.3 Triple-layered panels

Multi-layered plates, including three layers of steel, composite, and aluminum honeycomb, with total thicknesses between 16.7 mm and 22.1 mm, were designed to investigate the effect of layer configuration. A hybrid armor plate using Hardox steel could not be suggested, as even the 4H24K10B triple-layered armor construction could not exhibit ballistic success either. The front steel and rear aluminum honeycomb layers of the 4A24K10B sample failed due to petalling, whereas the intermediate Kevlar29/epoxy layer failed due to fiber breakage. The composite layer is fabricated in the armor plates using Armox 500T on the impact surface by increasing the aramid-epoxy layers from 6 to 18. The test results for the 4A6K10B, 4A8K10B, and 4A10K10B plates showed complete perforation. It can be said that the number of Kevlar layers in these samples didn't work. To provide enough frictional resistance to dissipate the energy of the bullet core. The 4A12K10B design has been confirmed to offer ballistic protection since it stops the bullet. The results indicated that increasing the Kevlar29/epoxy layer in multi-layer structures enhanced ballistic resistance.

On the other hand, adding an aluminum honeycomb to increase the overall layer thickness did not dramatically improve the perforation resistance. The 4A14K10B, 4A16K10B, and 4A18K10B plates exhibited ballistic protection. As the number of Kevlar layers decreased, complete perforation damage occurred. Ballistic resistance was offered as the number of Kevlar layers increased. In this case, the 4A12K10B plate, which has a weight advantage, is suggested for ballistic protection instead of the 6A plate. Figure 8a illustrates the residual velocities of the bullet penetrating hybrid eight configurations. As shown in the numerical results, the factor that induced the complete perforation of the hybrid plates was the removal of the particle from the steel plate. In the multi-layered samples, the rigid steel layer in front is well supported by the Kevlar 29/epoxy and aluminum honeycomb plates in the rear, which can be validated from the literature [32]. Therefore, the fragmentation failure mode occurred in the steel layer. With an

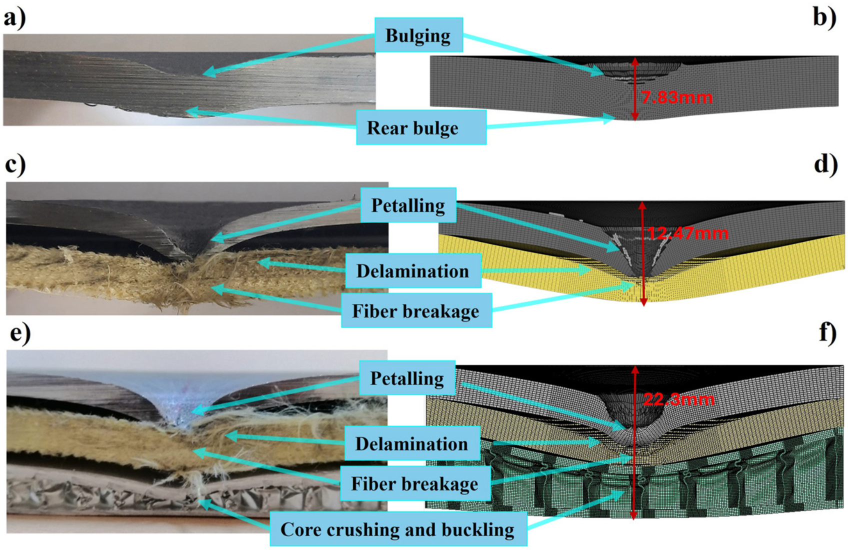

Figure 12: Permanent deformation values of plates providing ballistic protection a and b) 6A, c and d) 4A14K, e and f) 4A12K10B.

increase in the Kevlar layer's thickness, the 'velocity of the steel particles decreased. Figure 8b illustrates the velocity-time graphs of steel particles from armor plates subjected to complete perforation damage mode.

The visual of the damage caused by the ballistic test of the hybrid 4A12K10B plate is given in Figure 9. Following petalling damage to the Armox500T front steel plate, the Kevlar29/epoxy laminate experienced delamination damage and fiber breakage.

The rear aluminum honeycomb plate suffered buckling damage in the cell walls and core crushing in the impact zone. Figure 10 shows the post-impact fragmentation failure mode of the 4A10K10B plate with total perforation damage.

Figure 11 shows the Von Mises stress distribution of the 4A6K10B and 4A10K10B samples, representing the thinnest and thickest triple-layered panels subjected to total perforation by bullet impact. Introducing additional Kevlar29/epoxy layers resulted in higher stress values in the intermediate plate and decreased deformation in the back aluminum honeycomb plate. The Armox 500T and Kevlar29/epoxy plates in the 4A6K10B and 4A10K10B samples were entirely perforated, resulting in fragments from the steel tearing the aluminum honeycomb panel. In addition, the steel fragment induced severe damage to the face sheets of the honeycomb plate, resulting in further crushing and distortion of the cellular structures.

3.4 Comparison of best samples providing ballistic protection

The displacement amounts of the best panels exhibiting ballistic protection results in the direction of the bullet impact axis are as in Figure 12. Samples 6A (Figure 12a and b), 4A14K (Figure 12c and d), and 4A12K10B (Figure 12e and f) have thicknesses of 6 mm, 10.3 mm, and 19.4 mm, respectively.

Monolithic 6A steel had the lowest permanent deformation value; however, its area weights were higher. The areal density of the 6A sample is 7.83 kg m^{-2}, the 4A14K sample is 3.83 kg m^{-2}, and the 4A12K10B sample is 3.36 kg m^{-2}. Compared to the 6A sample, the 4A14K sample offers a 51 wt.% benefit, while the 4A12K10B sample provides a 57 wt.% advantage. Replacing the 6A with 4A14K and 4A12K10B double and triple-layered panels will be possible. There are differences in damage mechanisms among samples that absorb all bullet energy. The 4A14K sample had radial cracks on the rear surface of the front steel layer, while the Kevlar29/epoxy layer was not completely perforated. However, in the 4A12K10B sample, Armox 500T and Kevlar29/epoxy plates were perforated entirely, and the aluminum honeycomb panel stopped the fragments that broke off from the steel.

To clarify the results of the 20 samples, see Table 7. The comparison criteria between simulation and experiment results in the table are determined using the complete perforation condition, the bullet's remaining velocity after perforation, if there is one, and the armor plate's backface deformation.

For a better evaluation of the results considering the weight and ballistic performance, the specific energy absorptions of the best samples are also given in Table 8. As seen in Table 8, the 6A design is the thinnest choice; however, it cannot absorb much impact energy and can be regarded as being at the limit of ballistic resistance. It can be concluded that monolithic plates exhibit superior experimental performance; however, additional analysis using finite element analysis reveals that their energy absorption capacity is at its limit. Sample 4A12K10H has the

Table 7: Comparison between the experimental and simulation results.

Sample code	Muzzle velocity (m s^{-1})	FEM residual speed (m s^{-1})	Full perforation	Sample thickness (mm)	Back face deformation	
					Experiment (mm)	Simulation (mm)
4A	838 ± 15	544	Yes	4	–	–
4H		774	Yes	4	–	–
6A		–	No	6	1.10	1.12
6H		–	No	6	1.92	2.98
4A6K		506	Yes	6.70	–	–
4A8K		447	Yes	7.60	–	–
4A10K		430	Yes	8.50	–	–
4A12K		412	Yes	9.40	–	–
4A14K		–	No	10.30	1.20	1.24
4A16K		–	No	11.20	0.50	0.52
4A18K		–	No	12.10	0.43	0.44
4H24K		692	Yes	14.80	–	–
4A6K10B		355	Yes	16.70	–	–
4A8K10B		339	Yes	17.60	–	–
4A10K10B		258	Yes	18.50	–	–
4A12K10B		–	No	19.40	2.15	2.18
4A14K10B		–	No	20.30	1.78	1.82
4A16K10B		–	No	21.20	0.98	1.00
4A18K10B		–	No	22.10	0.81	0.82
4H24K10B		624	Yes	24.80	–	–

Table 8: Specific energy absorption (SEA) of the best samples.

Configuration	SEA (Joule kg^{-1})	Mass (kg)	Thickness (mm)
6A	244.54	3.19	6.00
4A14K	282.87	2.55	8.20
4A12K10H	502.10	2.88	17.60

highest SEA, but has the thickest panel, measuring 17.6 mm. The 4A14K sample is the optimum design since it is placed second in specific energy absorption while being 53 wt.% thinner and 11.5 wt.% lighter than the most impact-resistant 4A12K10H sample.

4 Conclusions

A parametric study on 20 different armor combinations, including four monolithic steel and sixteen multi-layered panels, evaluated their ballistic resistance numerically validated via an experimental approach. The armor combinations used against 7.62 × 51 mm full metal jacket bullet impacts at a muzzle velocity of 838 ± 15 m s^{-1} during the ballistic tests. The configurations were subjected to ballistic testing according to the NIJ STD-0101.08 Level III standard. The numerical models were tested to validate the experimental data from the literature, demonstrating a good agreement between the simulation results and the experimental findings. The following conclusions can be made from this research:

Monolithic thicker steel experienced bulge failure and showed less permanent deformation than multi-layer systems.

The 4 mm thick Hardox 450 steel combination with Kevlar29/epoxy laminate and aluminum honeycomb failed to protect the 7.62 × 51 mm FMJ bullet threat.

Double-layered 4A14K armor provides ballistic protection similar to thick steel 6 mm Armox 500T monolithic armor at a lower weight. Adding Kevlar 29/epoxy layers produced the formation of radial fractures and crack damage modes on the rear surface of the front steel plate, preventing total perforation.

Triple-layer 4A12K10B hybrid armor is more lightweight than 6A monolithic steel and offers equal ballistic protection. Using an aluminum honeycomb, the fragmenting effect induced complete perforation failure mode in triple-layered samples. Increasing the number of Kevlar29/epoxy layers prevented this situation.

Compared to the monolithic 6 mm Armox 500T panel, the double-layered 4A14K plate is 51 wt.% lighter in areal weight, while the triple-layered 4A12K10B panel is 57 wt.% lighter in areal weight. It is clear that 4A14K and 4A12K10B samples may be employed successfully in ballistic protection and have the potential to decrease area mass efficiency significantly.

A deeper investigation using FEA reveals that the honeycomb aluminum panel can be used on armored personnel vehicles and increases specific energy absorption capacity.

Future research aims to analyze the multi-layered armor configurations proposed in this work for their ballistic resistance against larger caliber and armor-piercing (AP) bullets.

Acknowledgments: The authors would like to thank ZSR Inc. (Balıkesir, Turkey) for allowing ballistic testing using their outdoor shooting ranges. The authors would like to thank "Numesys, Türkiye", the solution partner of Dr. Yılmazçoban's "IKY Research Group", for their support with Ansys and LS-DYNA.
Research ethics: Not applicable.
Informed consent: Not applicable.
Author contributions: MO: Conceptualization, Methodology, Software, Validation, Formal analysis, Investigation, Data curation, Writing – original draft, Writing – review & editing, KF: Software, Validation, Formal analysis, FB: Investigation, Data curation, Writing – review & editing, TKD: Investigation, Data curation, Visualization, IKY: Conceptualization, Supervision, Writing – review & editing, CC: Project administration, Conceptualization. Supervision.
Use of Large Language Models, AI and Machine Learning Tools: None declared.
Conflict of interest: The authors state there is no conflict of interest.
Research funding: This research was supported by Manisa Celal Bayar University Office of Scientific Research Projects (Türkiye) (Grant no. 2023/020).
Data availability: The raw data can be obtained on request from the corresponding author.

References

[1] F. J. Ramírez-Gil, E. C. N. Silva, and W. Montealegre-Rubio, "Through-thickness perforated steel plates optimized for ballistic impact applications," *Mater. Des.*, vol. 212, no. 110257, pp. 1–16, 2021, https://doi.org/10.1016/j.matdes.2021.110257.
[2] A. Yilmaz, "Development of an armor steel for ballistic protection," *Mater. Test.*, vol. 52, nos. 11–12, pp. 811–818, 2010, https://doi.org/10.3139/120.110190.
[3] A. K. Gur, S. Taskaya, S. Shankar, and T. Mohanraj, "FEA of SAW penetration of Ramor 500 steel," *Mater. Test.*, vol. 62, no. 12, pp. 1192–1198, 2020, https://doi.org/10.3139/120.111605.
[4] D. Lenihan, W. Ronan, P. E. O'Donoghue, and S. B. Leen, "A review of the integrity of metallic vehicle armour to projectile attack," *Proc. Inst. Mech. Eng. Part L J. Mater. Des. Appl.*, vol. 233, no. 1, pp. 73–94, 2019, https://doi.org/10.1177/1464420718759704.
[5] Z. Rosenberg and E. Dekel, *Terminal Ballistics*, Berlin, Springer, 2012.
[6] K. Senthil and M. A. Iqbal, "Prediction of superior target layer configuration of armour steel, mild steel and aluminium 7075-T651 alloy against 7.62 AP projectile," *Struct. Elsevier*, vol. 29, pp. 2106–2119, 2021, https://doi.org/10.1016/j.istruc.2020.06.010.
[7] A. Paman, G. Sukumar, B. Ramakrishna, and V. Madhu, "An optimization scheme for a multilayer armour module against 7.62 mm armour piercing projectile," *Int. J. Prot. Struct.*, vol. 11, no. 2, pp. 185–208, 2020, https://doi.org/10.1177/2041419619860533.
[8] L. Peng *et al*., "Investigations of the ballistic response of hybrid composite laminated structures," *Compos. Struct.*, vol. 282, no. 115019, pp. 1–17, 2022, https://doi.org/10.1016/j.compstruct.2021.115019.
[9] E. Palta, M. Gutowski, and H. Fang, "A numerical study of steel and hybrid armor plates under ballistic impacts," *Int. J. Solids Struct.*, vols. 136–137, pp. 279–294, 2018, https://doi.org/10.1016/j.ijsolstr.2017.12.021.
[10] A. Kraus, E. Kraus, and I. Shabalin, "Modelling of the processes of impact of a projectile with elements of individual defence," *EPJ Web Conf.*, vol. 221, no. 01021, pp. 1–10, 2019, https://doi.org/10.1051/epjconf/201922101021.
[11] K. Kartikeya, H. Chouhan, K. Ram, S. Prasad, and N. Bhatnagar, "Ballistic evaluation of steel/UHMWPE composite armor system against hardened steel core projectiles," *Int. J. Impact Eng.*, vol. 164, no. 104211, pp. 1–13, 2022, https://doi.org/10.1016/j.ijimpeng.2022.104211.
[12] S. Rathod, N. Khaire, and G. Tiwari, "A comparative study on the ballistic performance of aramid and aluminum honeycomb sandwich structures," *Compos. Struct.*, vol. 299, no. 116048, pp. 1–21, 2022, https://doi.org/10.1016/j.compstruct.2022.116048.
[13] N. Khaire, G. Tiwari, V. Patel, and M. Iqbal, "Assessment of the ballistic response of honeycomb sandwich structures subjected to offset and normal impact," *Def. Technol.*, vol. 28, pp. 56–73, 2023, https://doi.org/10.1016/j.dt.2022.12.018.
[14] Q. Zhang, X. Zhang, G. Lu, and D. Ruan, "Ballistic impact behaviors of aluminum alloy sandwich panels with honeycomb cores: an experimental study," *J. Sandw. Struct. Mater.*, vol. 20, no. 7, pp. 861–884, 2018, https://doi.org/10.1177/1099636216682166.
[15] K. Arslan, R. Gunes, M. K. Apalak, and J. Reddy, "Experimental tests and numerical modeling of ballistic impact on honeycomb sandwich structures reinforced by functionally graded plates," *J. Compos. Mater.*, vol. 51, no. 29, pp. 4009–4028, 2017, https://doi.org/10.1177/0021998317695423.
[16] J. Stewart, *Ballistic Resistant Protective Materials – NIJ Standard 0108.01*, Washington, National Institute of Justice, 1985.
[17] Armox 500T General Product Description, SAAB, 2016. [Online]. Available at: https://www.ssab.com/en/brands-and-products/armox/product-offer/armox-500t.
[18] D. S. Morghode, D. Thakur, S. Salunkhe, L. Cepova, and E. Abouel Nasr, "Analysis of the thickness of layered armor to provide protection against 7.62 mm ball projectiles using experimental and numerical methods," *Front. Mech. Eng.*, vol. 10, no. 1419210, pp. 1–18, 2024, https://doi.org/10.3389/fmech.2024.1419210.

[19] D. S. Morghode, D. Thakur, S. Salunkhe, L. Cepova, and E. Abouel Nasr, “Numerical study on the optimized thickness of layer configuration against the 7.62 APM2 projectile,” *Front. Mech. Eng.*, vol. 10, no. 1322640, pp. 1–16, 2024, https://doi.org/10.3389/fmech.2024.1322640.

[20] J. O. Hallquist, *LS-DYNA Theory Manual*, vol. 3, Livermore, CA, Livermore Software Technology Corporation, 2006, pp. 25–31.

[21] G. R. Johnson, “A constitutive model and data for metals subjected to large strains, high strain rates and high temperatures,” in *Proceedings of the 7th International Symposium on Ballistics, The Hague, Netherlands*, 1983.

[22] İ. Memis and R. Karakuzu, “High-velocity impact performance of Ramor 500 armor steel,” *Mater. Test.*, vol. 64, no. 7, pp. 991–1001, 2022, https://doi.org/10.1515/mt-2022-0035.

[23] M. Saleh, V. Luzin, M. M. Kariem, and D. Ruan, “Analysis of the residual stress in ARMOX 500T armour steel and numerical study of the resultant ballistic performance,” *Mater. Res. Proc.*, vol. 2, pp. 437–442, 2017. https://doi.org/10.21741/9781945291173-74.

[24] J. Hub and J. Komenda, “Ballistic’s resistance of steel plate hardox upon impact of non penetrating projectiles,” *Adv. Mil. Technol.*, vol. 4, no. 2, pp. 79–91, 2009.

[25] H. Gower, D. Cronin, and A. Plumtree, “Ballistic impact response of laminated composite panels,” *Int. J. Impact Eng.*, vol. 35, no. 9, pp. 1000–1008, 2008, https://doi.org/10.1016/j.ijimpeng.2007.07.007.

[26] S. Kumar, D. S. Gupta, I. Singh, and A. Sharma, “Behavior of Kevlar/epoxy composite plates under ballistic impact,” *J. Reinf. Plast. Compos.*, vol. 29, no. 13, pp. 2048–2064, 2010, https://doi.org/10.1177/0731684409343727.

[27] J.-H. Ahn, K.-H. Nguyen, Y.-B. Park, J.-H. Kweon, and J.-H. Choi, “A numerical study of the high-velocity impact response of a composite laminate using LS-DYNA,” *Int. J. Aeronaut. Space Sci.*, vol. 11, no. 3, pp. 221–226, 2010, https://doi.org/10.5139/IJASS.2010.11.3.221.

[28] S. Feli and M. Asgari, “Finite element simulation of ceramic/composite armor under ballistic impact,” *Compos. B: Eng.*, vol. 42, no. 2, pp. 771–780, 2011, https://doi.org/10.1016/j.compositesb.2011.01.024.

[29] L. M. Bresciani, A. Manes, A. Ruggiero, G. Iannitti, and M. Giglio, “Experimental tests and numerical modelling of ballistic impacts against Kevlar 29 plain-woven fabrics with an epoxy matrix: Macro-homogeneous and Meso-heterogeneous approaches,” *Compos. B: Eng.*, vol. 88, pp. 114–130, 2016, https://doi.org/10.1016/j.compositesb.2015.10.039.

[30] M. K. Dewangan and S. Panigrahi, “FEA of plain woven Kevlar/epoxy composites subjected to normal and oblique impact with multi-scale modelling,” *Fibers Polym.*, vol. 21, pp. 2927–2937, 2020, https://doi.org/10.1007/s12221-020-0089-0.

[31] B. Tepeduzu and R. Karakuzu, “Ballistic performance of ceramic/composite structures,” *Ceram. Int.*, vol. 45, no. 2, pp. 1651–1660, 2019, https://doi.org/10.1016/j.ceramint.2018.10.042.

[32] I. Yilmazcoban and S. Doner, “Ballistic protection evaluation of sequencing the composite material sandwich panels for the reliable combination of armor layers,” *Acta Phys. Pol. A*, vol. 130, no. 1, pp. 342–346, 2016, https://doi.org/10.12693/APhysPolA.130.

The authors of this contribution

Mehmet Özer

Dr. Mehmet Özer was born in 1979 and graduated from Balıkesir University in Balıkesir, Turkey in 2002 with a bachelor’s degree in Mechanical Engineering. He completed his doctoral studies at Manisa Celal Bayar University in Manisa province and received his doctorate degree in 2025. He is currently working as a Dr. Lecturer at Balıkesir Vocational School of Balıkesir University in Turkey. His research focuses on 3D printing, composite materials, and ballistic resistance.

Fatih Balıkoğlu

Dr. Fatih Balıkoğlu, born in 1982, studied Mechanical Engineering at the “Engineering Faculty, Balıkesir University, Türkiye”. He completed a doctoral study in the Mechanical Engineering Department. He has been working as an Associate. Prof. Dr. at Balıkesir University, Mechanical Engineering Department. Dr. Fatih Balıkoğlu works in the fields of polymer composites, experimental mechanics, and the mechanics of composite materials.

Tayfur Kerem Demircioğlu

Dr. Tayfur Kerem Demircioğlu, born in 1980, studied Mechanical Engineering at the “Engineering Faculty, Balıkesir University, Türkiye”. He completed a doctoral study in the Mechanical Engineering Department. He has been working as an Assist. Prof. Dr. at Balıkesir University, Mechanical Engineering Department. Dr. Tayfur Kerem Demircioğlu works in the fields of composite materials, the computer aided design, and analysis.

Can Çivi

Dr. Can Çivi, born in 1987, graduated from Manisa Celal Bayar University in 2009 with a degree in mechanical engineering. He completed a Master of Science and doctoral studies in the Mechanical Engineering Department. He has been working as an Associate. Prof. Dr. at Manisa Celal Bayar University, Mechanical Engineering Department. Dr. Can ÇİVİ works in machine design, material development, and examination of the mechanical behavior of materials.

İbrahim Kutay Yilmazçoban

Dr. İbrahim Kutay Yilmazçoban, Dr. IKY, was born in 1977. He got his B.S. degree from The Mechanical Eng. Dept. Sakarya University, in 2000 and his M.Sc. in 2003. His Ph.D. in “the numerical explicit investigation for the frontal impacts of the wheelchairs and vehicles” was also defended at the Sakarya University in 2009. He was accommodated as an Assistant Prof. in the same department after he finished his Ph.D He is still a faculty member at Sakarya University.